In Situ Controllable Loading of Ultrafine Noble Metal Particles on Titania

Yun Xie, Kunlun Ding, Zhimin Liu,* Ranting Tao, Zhenyu Sun, Hongye Zhang, and Guimin An

Beijing National Laboratory for Molecular Science, Institute of Chemistry, Chinese Academy of Sciences, Beijing 100190, China

Received January 20, 2009; E-mail: liuzm@iccas.ac.cn

Noble metal-loaded titania composites have received much attention for decades. They have been found to have wide applications from photochemistry to heterogeneous catalysis due to their unique features originating from the combination of a catalytically active noble metal and a key semiconductor material.[1] Numerous studies have found that the properties of these kind of composites are strongly dependent on the metal particle size, dispersion, and composition, etc.[2] Especially, as the sizes of metal particles fall below 2.0 nm, the composites display exceptional catalytic behavior.[3] Therefore, it is significant to prepare metal loaded TiO_2 nanocomposites with homogeneous metal dispersion, tunable (especially ultrafine) metal particle size, and narrow particle size distribution.

In recent years, several approaches for the preparation of noble metal/TiO_2 composites have been reported, including conventional impregnation and deposition−precipitation (DP) techniques, photodepositon, sputtering, colloidal methods, and so on.[4] The classical methods of impregnation and DP are relatively simple but allow poor control over the particle size, dispersion, and composition. The other approaches give better ways to tune these factors; however, they suffer from their inherent drawbacks. Thus it is still desirable to develop simple and effective approaches to synthesize metal/TiO_2. Especially, controllably loading metal clusters with a size less than 2.0 nm on TiO_2 is of importance and a challenge.

Herein, we present a novel, simple, and clean method to grow directly noble metal particles on titania through an in situ redox reaction between the reductive titanium(III) oxide support and metal salt precursors in aqueous solution. This method has the following obvious advantages: (i) the metal particles are uniformly distributed on the TiO_2 support, and their average size can be mediated from ∼0.5 to ∼2.5 nm with a very narrow size distribution; (ii) no extra reducing agent is required, avoiding introduction of impurity; (iii) the method can be operated under mild conditions. We believe that this approach can be extended to the synthesis of other metal/metal oxide composites.

We used $TiCl_3$ and noble metal salts as the starting materials, and detailed information for the synthesis and characterization of the TiO_2 supported nanocomposites is included in the Supporting Information. In this method, the titanium(III) oxide nanostructure was first formed via $TiCl_3$ hydrolysis in acidic aqueous solution containing excessive Cl^-, which had a strong reducing ability. Once the metal ions were in contact with the titanium(III) oxide nanostructure in aqueous solution, they were immediately reduced by the support and nucleated rapidly on its surface to grow into clusters and further into nanoparticles. Meanwhile, the support was partially oxidized by the metal ions and further converted completely into TiO_2 after exposure to air, resulting in metal/TiO_2 nanocomposites. A two-step injection was used to introduce a metal precursor in this method. Due to the rapid nucleation on titanium(III) oxide, a large amount of ultrafine nuclei in situ formed on the support as the first portion of the precursor was injected, which served as seeds for the growth of the metal particles as more precursor

was introduced. Changing the total amount of the precursor and the mass ratio of the first and the second added precursor, the metal particle size and loading content can be readily tuned. Especially, the metal/TiO_2 composites with the same metal content but different particle size and composites with the same particle size but different metal content can be controllably prepared.

Transmission electron microscopy (TEM) observation showed that in all as-prepared samples TiO_2 was displayed as nanorods with a diameter of 10−50 nm and length of ∼200 nm, which was the rutile phase confirmed by XRD analysis (JCPDS, No. 21-1276, Figure S1). The metal/TiO_2 composite with a metal content of A wt% and mean metal particle size of B nm is denoted as metal/TiO_2 (A wt%, B nm). Figure 1a shows a typical scanning TEM
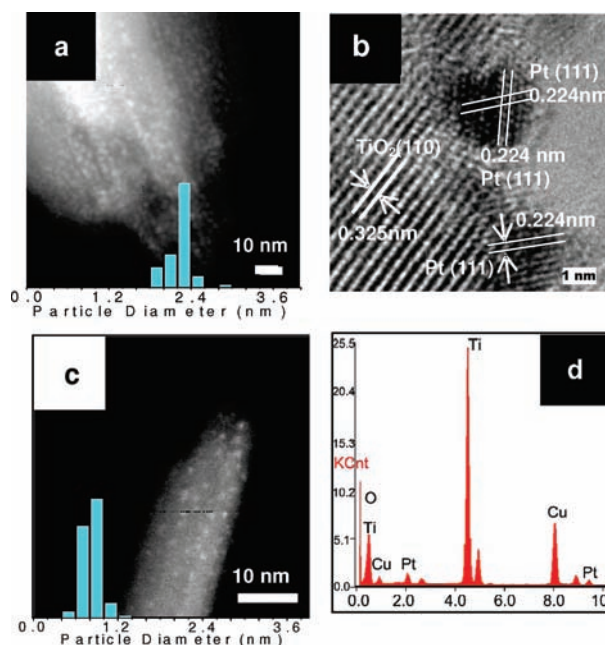
Figure 1. STEM image and particle size distribution (a) and HRTEM image (b) of Pt/TiO_2 (2.93 wt %, 2.3 nm), STEM image and particle size distribution (c) and EDS spectrum (d) of Pt/TiO_2 (1.24 wt %, 0.9 nm).

(STEM) image of a Pt/TiO_2 (2.93 wt %, 2.3 nm) composite, which clearly displays the homogeneous Pt deposit throughout the TiO_2 support. Energy-dispersive spectroscopy (EDS) analysis during the TEM observation for many different regions also confirmed the uniform dispersion of Pt species on the support. High-resolution TEM (HRTEM) analysis (Figures 1b and S2) revealed the highly crystalline features of the support as well as Pt particles. The fringes with a lattice spacing of 0.224 nm can be indexed as the (111) plane of face-centered cubic (fcc) Pt, and the angle between two Pt (111) planes also perfectly agrees with the fcc Pt. This suggests that titanium(III) oxide had enough reducing ability to convert the

Pt precursor into Pt. The Pt/TiO$_2$ (1.24 wt %, 0.9 nm) composite also exhibited a similar morphology (Figure 1c); however, the lattice space of the particles could not be observed probably due to their tiny size. To the best of our knowledge, a uniform dispersion of ultrafine nanoparticles onto the entire region of the TiO$_2$ support was realized for the first time. It is worth noting that the Pt particle size could be mediated from ~0.5 to ~2.3 nm (see Figures S2−6), while the metal content could be tuned to different levels. Particularly, the Pt/TiO$_2$ composites with a high Pt content (e.g., 2.44 wt %) and an ultrafine average particle size (e. g., 0.5 nm) were obtained (see Figure S6).

The XRD profile of Pt/TiO$_2$ (1.24 wt %, 0.9 nm) (Figure S1) only shows the diffraction of the support and no characteristic Pt diffraction, implying the very small size of the Pt particles. X-ray photoelectron spectra (XPS) of this sample together with samples Pt/TiO$_2$ (2.93 wt %, 2.3 nm) and Pt/TiO$_2$ (2.44 wt %, 0.5 nm) show obvious peaks of Pt with a Pt $4f_{7/2}$ apparent binding energy (BE) of ~72.5 eV (see Figures S7−9), which were higher than that of the bulk Pt (71.2 eV). In addition, the Cl element was detectable for these three samples, which might increase the BE of the Pt cluster. It is well-known that the core level BE of a metal cluster increases with reduced cluster size.[3,5] The Pt 4f BE of Pt clusters could even increase by 1.0−2.0 eV.[6] In this work, the shift of the Pt $4f_{7/2}$ BE to a higher value might be attributed to the effects of the Pt cluster size and a trace amount of Cl$^-$ ions adsorbed on the samples. The Ti 2p signals (see Figure S8) were highly symmetric, and no shoulders appeared at the lower energy side of the Ti 2p signals, suggesting that the defect concentration associated with Ti^{3+} was extremely low; that is, nearly all the titanium(III) oxide was oxidized to TiO$_2$.

The UV−visible diffuse reflectance spectra of the Pt/TiO$_2$ composites (see Figure S10) indicated a unique size-dependent surface plasmon resonance effect,[7] and the absorbance red-shifted with Pt cluster size from ~0.5 to ~1.4 nm. It has been widely accepted that Pt particles deposited on TiO$_2$ can suppress the recombination of electron−hole pairs in TiO$_2$, where the Pt particles act as electron traps aiding electron−hole separation. Three Pt/TiO$_2$ samples with a Pt particle size less than 1.0 nm were used to degrade phenol. Under dark conditions no reaction was observed even after 6 h, while under UV irradiation all of the Pt loaded titania displayed dramatically improved photodegradation efficiency compared to the naked TiO$_2$ nanorods (see Figure S11). Interestingly, Pt/TiO$_2$ (2.44 wt %, 0.5 nm) showed the highest efficiency for this reaction, which could almost completely degrade phenol within 1 h. The significantly enhanced activity should result from the strong synergy between the nanostructured TiO$_2$ support and tiny Pt particles.

We also prepared Au/TiO$_2$, Ru/TiO$_2$, and PtRu/TiO$_2$ composites using the method described above. Figure 2 illustrates TEM images of these samples, which displays that numerous particles with an ultrafine size and a very narrow size distribution were decorated on the surface of TiO$_2$ nanorods. We examined the activity of the PtRu/TiO$_2$ composites for degrading phenol under UV irradiation and found that they were also highly active for this reaction. For example, PtRu/TiO$_2$ (0.52 wt % Pt, 0.13 wt % Ru, 1.0 nm) could convert 90% of phenol within 3 h (see Figure S11).

In conclusion, we have developed a novel and simple method to in situ load noble metals on TiO$_2$. Through a redox reaction between the reductive titanium(III) oxide support and metal salt precursors, a series of noble metal/TiO$_2$ nanocomposites with
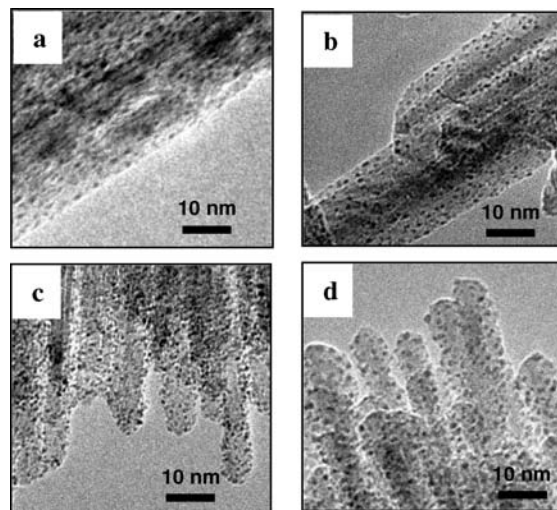
Figure 2. TEM images of metal/TiO$_2$ composites: (a) Au/TiO$_2$ (0.62 wt %, 1.0 nm), (b) Ru/TiO$_2$ (0.71 wt %, 0.7 nm), (c) PtRu/TiO$_2$ (0.37 wt % Pt, 0.13 wt % Ru, 0.7 nm), (d) PtRu/TiO$_2$ (0.52 wt % Pt, 0.13 wt % Ru, 1.0 nm).

uniform metal dispersion, tunable metal particle size, and narrow metal particle size distribution were obtained. This method may open up a new way to prepare metal supported composites. The as-prepared metal/TiO$_2$ nanocomposites have promising applications in catalysis, which are expected to effectively catalyze some reactions under low temperature. A study on their catalytic activity for different chemical reactions is underway in our laboratory.

Supporting Information Available: Preparation and characterization (XRD, TEM, XPS, UV−visible diffuse reflectance spectra, photocatalytic activity test) of metal/TiO$_2$ nanocomposites. This material is available free of charge via the Internet at http://pubs.acs.org.

References

(1) (a) Valden, M.; Lai, X.; Goodman, D. W. *Science* **1998**, *281*, 1647. (b) Enache, D. I.; Edwards, J. K.; Landon, P.; Solsona-Espriu, B.; Carley, A. F.; Herzing, A. A.; Watanabe, M.; Kiely, C. J.; Knight, D. W.; Hutchings, G. J. *Science* **2006**, *311*, 362. (c) Li, H. X.; Bian, Z. F.; Zhu, J.; Huo, Y. N.; Li, H.; Lu, Y. F. *J. Am. Chem. Soc.* **2007**, *129*, 4538. (d) Hirakawa, T.; Kamat, P. V. *J. Am. Chem. Soc.* **2005**, *127*, 3928. (e) Zukalova, M.; Zukal, A.; Kavan, L.; Nazeeruddin, M. K.; Liska, P.; Gratzel, M. *Nano. Lett.* **2005**, *5*, 1789.
(2) Chen, M. S.; Goodman, D. W. *Acc. Chem. Res.* **2006**, *39*, 739. (b) Corma, A.; Serna, P.; Garca, H. *J. Am. Chem. Soc.* **2007**, *129*, 6358.
(3) Turner, M.; Golovko, V. B.; Vaughan, O. P. H.; Abdulkin, P.; Berenguer-Murcia, A.; Tikhov, M. S.; Johnson, B. F. G.; Lambert, R. M. *Nature* **2008**, *454*, 981.
(4) (a) Lin, C. H.; Chao, J. H.; Liu, C. H.; Chang, J. C.; Wang, F. C. *Langmuir* **2008**, *24*, 9907. (b) Yan, W. F.; Shannon, M. M.; Pan, Z. W.; Steven, H. O.; Dai, S. *J. Am. Chem. Soc.* **2005**, *127*, 10480. (c) Chen, J. I. L.; Loso, E.; Ebrahim, N.; Ozin, G. A. *J. Am. Chem. Soc.* **2008**, *130*, 5420. (d) Albers, P.; Seibold, K.; McEvoy, A. J.; Kiwi, J. *J. Phys. Chem.* **1989**, *93*, 1510. (e) Li, J.; Zeng, H. C. *Chem. Mater.* **2006**, *18*, 4270.
(5) Wertheim, G. K.; DiCenzo, S. B. *Phys. Rev. B* **1988**, *37*, 844.
(6) Eberhardt, W.; Fayet, P.; Cox, D. M.; Fu, Z.; Kaldor, A.; Sherwood, R.; Sondericker, D. *Phys. Rev. Lett.* **1990**, *64*, 780.
(7) Bigall, N. C.; Hartling, T.; Klose, M.; Klose, M.; Simon, P.; Eng, L. M.; Eychmuller, A. *Nano. Lett.* **2008**, *8*, 4588.

JA900447D